Estimation of the advection effects induced by surface heterogeneities in the surface energy budget

J. Cuxart[1], **B. Wrenger**[2], **D. Martínez-Villagrasa**[1], **J. Reuder**[3], **M.O. Jonassen**[3], **M.A. Jiménez**[1], **M. Lothon**[4], **F. Lohou**[4], **O. Hartogensis**[5], **J. Dünnermann**[2], **L. Conangla**[6], and **A. Garai**[7]

[1]Universitat de les Illes Balears, Palma (Mallorca, Spain)
[2]Hochschule Ostwesfalen-Lippe, Höxter (Nordrhein-Westfalen, Germany)
[3]Geophysical Institute, University of Bergen (Norway)
[4]Centre Recherches Atmospheriques, Univ. Toulouse & CNRS, Lannemezan (France)
[5]Wageningen University of Research (The Netherlands)
[6]Universitat Politècnica de Catalunya, Manresa (Catalonia, Spain)
[7]University of California, San Diego (California, USA)

Correspondence to: J.Cuxart (joan.cuxart@uib.cat)

Abstract. The effect of terrain heterogeneities in one-point measurements is a continuous subject of discussion. Here we focus on the order of magnitude of the advection term in the equation of the temperature as generated by documented terrain heterogeneities and we estimate its importance as a term in the surface energy budget (SEB). The heterogeneities are estimated from satellite and model fields for scales near 1 kilometer or broader, while the smaller scales are estimated through direct measurements with remotely-piloted aircraft, thermal cameras and also by high-resolution modeling. The variability of the surface temperature fields is not found to decrease clearly with increasing resolution, and consequently the advection term becomes more important as the scales become finer. The advection term provides non-significant values to the SEB at scales larger than few kilometers. On the contrary, surface heterogeneities at the meter scale yield large values of the advection, which are probably only significant in the first centimeters above the ground. The motions that seem to contribute significantly to the advection term in the SEB equation in our case are roughly those around the hectometer scales.

1 Introduction

The Surface Energy Budget (SEB) is the expression of the conservation of energy for a volume across the atmosphere-surface interface, which should take into account all the energy exchanges taking place in it. Traditionally (see e.g. Oke, 1987, or Foken, 2008a, 2008b) it is expressed as an equilibrium equation between the Net Radiation (Rn) -usually the larger term- and the three other principal terms, the turbulent sensible heat flux (H), the latent heat flux (LE) and the soil heat flux (G). Conceptually it is computed for a layer of infinitesimal depth across the interface in a horizontally homogeneous area, therefore no storage or source terms are considered and, formally, the budget is expressed as

$$Rn + H + LE + G = 0 \tag{1}$$

where a possible criterion for the signs is that they are positive if they are directed towards the surface. This approach, when brought to the experimental field, implies a number of practical difficulties, which we may reduce to two major issues. Firstly the impossibility of measuring actually in a differential volume at the interface. As Foken (2008a) exemplifies, each instrument is measuring signal corresponding to a different volume of air. One way to overcome this conceptual difficulty is to acknowledge that we measure in a volume limited by the position of the instruments used. This implies that we must account for

storages and look for the divergence of the heat fluxes across the volume of measurement. Besides, the heat sources and sinks of energy within the volume must also be included (such as the energetic effects of biologic and anthropic activities).

The second main point comes from the fact that the emerged Earth surface is not homogeneous. If a researcher wanted to check the validity of equation (1), he should look for flat homogeneous locations, therefore distant from topographical features (even minor ones) or from changes in the soil uses (like different crops close to each other). These terrain heterogeneities may induce turbulent eddies and change the values of the turbulent heat flux compared to a completely homogeneous area.

The need of the scientific community to make experimental measurements, even in complex terrain, implies that these limitations should be progressively overcome. Nevertheless, Foken (2008b) acknowledged that, to progress in our understanding of the physics of the surface-atmosphere exchange, we must resign ourselves to work with imbalances of the order of 20% in Equation (1).

Cuxart et al (2015) derive a complete SEB equation from the evolution equation of the temperature of a volume. They take a conceptual box with the top at the screen level and the bottom just under the surface. Simplifying the equation accordingly, they produce a budget equation for the volume where the turbulent fluxes are located at screen level, the conduction flux just under the surface, the advection terms can be computed using the divergence of temperature across the volume limits and the missing terms can be accounted for explicitly if the information is available (see Figure 1 in that paper). Their rationale leads to an extended SEB equation:

$$Rn + H + LE + G + S + B + TT + A + Ot = 0 \tag{2}$$

where each term is considered at its own position relatively to the interface. Here S stands for the effect of the sources and sinks in the volume, including the storage in the mass elements and B the energy exchanges linked to the biologic and anthropic process. TT is the tendency of the temperature and A describes the effect of the advection term, presumably linked to the heterogeneities of the surface. The term Ot represents any other effect not accounted for in the budget, including the instrumental errors.

This approach is still insufficient because it implies several oversimplifications, such as not considering the internal variability of the volume (in the air and in the soil) or some inputs from outside the volume, such as water pumped up from below by the plant roots, all of it gathered into Ot, which is not estimated. Nevertheless it accounts explicitly for some elements of the imbalance, trying to progress with some insight in the SEB approach used in many practical environmental applications.

The total imbalance is expressed by Cuxart et al (2015, eq. 7) as the sum of the contributions of the tendency, the storage, the biological processes, the advection effects and the other unaccounted factors ($Imb = TT + A + S + B + Ot$). The imbalance values using long term averages is usually between 10% of the net radiation in flat homogeneous conditions (Oncley et al, 2007), increasing with the terrain complexity up to more than 30%. For individual averages of some minutes, the values can become much larger.

In this work we concentrate on the importance of the advection term A in the SEB. which represents the effect of the motions of timescales longer that the turbulence-averaged ones. Short-lasting surface temperature homogeneities induce eddy motions that are, in essence, turbulent, and therefore just treated statistically. If the inhomogeneities are lasting significantly longer that the averaging time to compute the turbulent fluxes then, by construction from the Reynolds decomposition, their effect has to be taken into account by the advection term. The latter may be expressed as (in W m^{-2})

$$A = \rho Cp \Delta z \sum_{i=1}^{3} u_i \frac{\Delta T}{\Delta x_i} \tag{3}$$

The related timescale must be the one used for the computation of the other terms in the budget. If 30-minute averages are used for the radiation or the turbulent heat fluxes, then the increments of temperature must be computed using 30-minute averages of temperature.

The term has some arbitrariness, especially in the value that must be taken for the dimensions of the box Δx_i. We will consider here thermal surface heterogeneities that last significantly longer than the characteristic times of the turbulence so that they can be treated as persistent thermal surface patterns generating durable circulations near the surface. It is unclear which are the scales contributing to the term without being distorted by obstacles between the station site and the different heterogeneities under consideration, as it is discussed in Leuning et al (2012).

The BLLAST experiment (Lothon et al, 2014) provided the opportunity of gathering several teams with different experimental and modeling expertises at the Lannemezan Plateau (Gascony, France) in summer 2011. In this work we analyze together a number of data from different sources operating during BLLAST with the aim of estimating the order of magnitude of A.

A number of simplifications is made to treat together such an heterogeneous amount of information. We will refrain our estimations of A to providing the order of magnitude of the term, taking 1 m s^{-1} as the characteristic wind speed at 2m above ground level (a.g.l.) for the analyzed events, which is a good approximation for the observed values (not shown). The concept of footprint is not used in this work, because the area is composed of patches of different land-use with a characteristic size of 100 m in all directions and this approach would be of difficult implementation considering averages of 30 minutes (for a discussion see Foken and Leclerc (2004) or, more recently, Hartogensis, 2015). The average vertical wind speed is taken as zero, acknowledging that this implies neglecting the vertical advection, therefore implicitly included in the Ot term. Finally the concept of blending height is only used sporadically since, as Foken (2008a) indicates, it may be not very appropriate when analyzing the effects of heterogeneity at relatively small scales.

In Section 2 the different sources of information are described, highlighting their potentialities and limitations. This is followed in Section 3 by a description of the SEB for the period 30 June-3 July and an analysis of the method. Section 4 provides a short description of the estimates of A for scales of the order of the kilometer to those of the order of the meter. In Section 5 an overall discussion of the findings is given before presenting the conclusions in Section 6.

2 Tools

During BLLAST a large number of teams contributed with instrumentation. Besides the main purpose of the experiment (the late afternoon and the evening transition regimes), there were a few other experiments in place (Lothon et al, 2014). One of them is treated in this paper, to see what may be the effect of small-scale terrain heterogeneities in the boundary layer. Ideally one should compare a perfectly homogeneous location with an inhomogeneous one, the former being actually very difficult to find over land, at least in mid-latitudes. The approach taken here, as described in the Introduction, is to use the available data to estimate the value of the advection term corresponding to the existent heterogeneities as detected by the different measuring devices.

BLLAST had two supersites, in site 1 there were vertical profiling devices, including radiosondes, and a number of surface layer measurements, some intended to assess the effect of the surface heterogeneities. Site 2 was intended to study well defined heterogeneities measuring over corn, moor and forest sites, each of an approximate scale of 1 km, larger than the average heterogeneities on the Lannemezan Plateau (van de Boer et al, 2014). The small-scale experiment under analysis here took place in site 1.

A complete SEB station was installed by the universities of Bergen and the Balearic Islands over a square of 160 m side over which there was a radar that was later moved to a nearby location. This "small square" is at a first look approximately flat and homogeneous, but a closer inspection shows that there is a very smooth slope towards SW and that the vegetation cover is irregular, some small areas being covered by grass and dead grass, others are bare and most of them are a mixture of short grass and bare soil.

The small square was surrounded by areas of grass for cattle, some wooden spots and fields of different crops, essentially the same landscape surrounding the area for several kilometers, with the exception of the city area of Lannemezan. The average scale of each of these landscape units was a few hundreds of meters at most, and most typically they had 100 m of characteristic size.

The BLLAST campaign was characterized by the passage of weather fronts approximately each third or fourth day, with clear skies and weak pressure gradients in between, when the wind dynamics over the Lannemezan plateau were dominated by the upvalley and downvalley circulations from the nearby Vallée d'Aure (Jiménez and Cuxart, 2014). Therefore the moisture availability at the surface was high, resulting in large daytime evapotranspiration fluxes (Bowen ratios below 1). We will focus in this work on the anticyclonic period between the rainy events of June 29 and July 3, which includes three BLLAST Intensive Observational Periods.

2.1 Measurements in the small square

Surface Energy Budget station: In the small square, the SEB consisted in i) the full radiation balance (Kipp and Zonen CNR1), ii) the sensible and latent heat fluxes with a Campbell integrated system that includes a CSAT-3 sonic anemometer and a Licor-7500 fast open-path CO2 and water vapor concentration sensor, iii) three Hukseflux ground soil flux plates and, iv) intermittently, a vertical array of eight thermocouples in the first two meters above the surface.

Upper soil moisture content: From June 21st to July 2nd manual measurements of the upper 5 cm of the soil moisture were made at selected spots (30, separated roughly 30 m on distinct areas, such as grass, half bare or short natural vegetation) within the small square once per day during Intensive Observing Periods. The sensors were Delta-T ML3 with a 1% accuracy. At each spot several measurements (typically 5) were taken in an area of 2m of radius due to the high variability of the measurements

and the final data for each spot was the average value. Due to the gentle slope towards SW, the western and southern sides, that
covered about one fourth of the small square, were flooded after a rainy event and a dry/wet homogeneity existed in the square,
since these areas had always larger soil moisture then the other ones.

Multicopter: From 1 to 5 July, a team of the Hochschule Ostwestfalen-Lippe operated a remotely-piloted multicopter
(Wrenger et al, 2013) over the small square, making 27 transects following a defined pattern that covered most of the well-
defined land-use areas, at a height near 7 m a.g.l. In a limited number of cases profiles up to 50 m were made over some points.
Here we use only the air temperature data -as sampled by a fast thermocouple supplemented with a slower Sensitron SHT75
sensor- and the surface temperature, provided by a factory-calibrated sensor Melexis MLX90614. The IR sensor had a view
angle of 35° implying a resolution circa 5 m if the sensor is vertically looking and degrading to circa 10 m when the flight was
slightly tilted in respect to the horizontal.

Multispectral camera of UCSD: A multispectral camera of the University of California at San Diego (Garai and Kleissl,
2013) was mounted at a height of 50 m agl in the 60-m tower close to the NW of the square. It was pointing to the square from
June 30 and was able to produce fields of surface temperature of the NW portion of the square with a time resolution of 1s, a
spatial resolution of 0.38 m × 0.18m with field of view 92m × 52m. The rated accuracy is 0.08 K.

Multispectral camera of WUR: On June 21, a team of the Wageningen University measured surface temperature with a
thermal camera on several areas of the small square producing high-resolution (centimeter scale) fields. The sensor was a IR
Snapshot camera from Infrared Solutions, producing images with 120 x 120 pixels and a field of view of 17 degrees. Each
field was for a rectangle of approximately 3 x 2 m^2. The procedure took a couple of hours, it started at mid-afternoon with
clear skies and ended an hour before sunset, with overcast skies that brought rain shortly after.

2.2 Measurements, model and satellite estimations at hectometer and larger scales

SUMO: The Small Unmanned Meteorological Observer (Reuder et al., 2009; Reuder and Jonassen, 2012) is a small (0.8 m of
wingspan) remotely controlled aircraft that was operated by the University of Bergen. For the purposes addressed here, it was
flown at an approximate height of 65 m a.g.l., over a squared area roughly of 1.6 km of side. The small square is about one-
hundredth part of the total area of the "SUMO square". The flights followed a grid pattern and, although each flight covered a
slightly different area, the small square area was always included. Here only temperature data are used. The air temperature was
measured by a Sensirion SHT 25 sensor, mounted inside a radiation protection tube on the wing, while the surface temperature
was estimated with a MLX90247 IR sensor, which had an angle of view circa 90°, with an effective resolution at the ground
close to 100 m. The typical ground speed was near 10 m s^{-1}.

Meso-NH: The simulation outputs of this non-hydrostatic model (Lafore et al, 1998) are used. The run was from June 29th at
0000 UTC to July 3rd at 0000 UTC, using three domains (Figure 1), with the same physical options and vertical discretization
as the simulation for the same area done in Jiménez and Cuxart (2014). The external domain (D1) covers the SW part of France,
including the Pyrenees and the Western valleys of the Massif Central, at a resolution of 2 km. The second domain (D2) is over
the Central Pyrenees and the plain at the foothills with a resolution of 400 m, while the inner domain (D3) has a resolution of
80 m, and is centered over the small square covering approximately the Lannemezan Plateau. D2 was only run between 1800
UTC of July 2n to 1000 UTC of July 3rd, and D3 only between 0000 UTC and 1000 UTC of July 2nd, conditioned by the
available computational resources.

The model uses a standard turbulence 1.5 order scheme (Cuxart et al, 2000), the ISBA soil scheme (Noilhan and Planton,
1989) and the radiation scheme of Morcrette (1990) as the more relevant parameterizations. It is initialized with the analysis of
the ECMWF for June 29 at 0000 UTC and is run until 0000 UTC of July 3, with lateral boundary conditions provided as well
by the ECMWF. A sponge layer is activated at its top. The numerical estimations of the surface temperature field and of the air
temperature at different heights are used.

Satellite data: The cloud-free areas of the satellite images from the MODIS sensor (Salomonson et al., 1989) onboard
the Terra and Aqua polar orbit satellites, available between June 30 and July 3, 2011 for SW France, are used to compute
the standard deviation of the surface temperatures as estimated by these radiometers with a resolution at this latitude circa 1
km. In very stable conditions, surface temperature may present some uncertainties (Martínez et al, 2010), mostly related to
condensation and frost in the surface elements, that may change their emissivity values. Meteosat second-Generation (MSG,
Schmetz et al, 2002) data at a resolution near 5 km is also used to provide time series of average Land Surface Temperature
(LST) and its standard deviation with a time resolution of 15 minutes. Contrarily to MODIS images, MSG surface temperature
is not corrected for atmospheric water vapor.
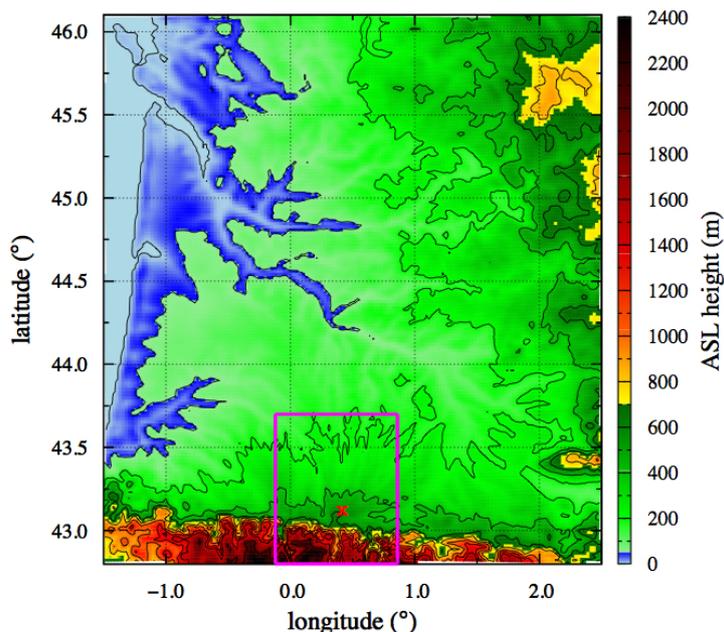
Figure 1. Topography of the southwestern part of France which corresponds to the larger domain of the model simulation (D1). The inner area inside a purple square corresponds to domain D2. The red cross indicates the location of Lannemezan, around which the domain D3 is taken (not shown). Areas for which the average LST and its standard deviation given in Figure 3 are computed are those in green for model domains D1 and D2.

2.3 Treatment of the advection term

As a first guess, it will be assumed that the depth of the volume for which the SEB will be computed is 2 m, since this is the typical distance between measurements at the surface layer and at the ground, that allow to compute vertical divergences. The horizontal dimension of the box will be the subject of this work, since we will explore what would be the contribution of the advection term to the budget depending on the horizontal scale of the thermal heterogeneity. It is clear that these computations will be rough estimates of the effect of the advection in the SEB, but it may provide a way of continuation.

For simplification purposes we will i) neglect here the vertical advection (taking $w = 0$ in average is reasonable), implying that the error associated with the neglection of the vertical advection is included in the Ot term of the complete SEB; ii) consider the horizontal term only following the dominant direction of the wind, which will be taken as x and will allow to write the advection term in a simpler way, and iii) take the factor $\rho Cp \Delta z \, u \approx 2500 \; J(K \, m \, s)^{-1}$, where $\Delta z = 2$ m and u at 2 m a.g.l. is of the order of 1 m s^{-1} for these clear and not windy ABL cases, leading to an expression for the order of magnitude of the advection term:

$$O[A] \approx 2500 \frac{\Delta T}{\Delta x} \tag{4}$$

3 The measured Surface Energy Balance in the small square

The SEB is computed for the station in the small square for the period 30 June at 1200 UTC to 3 July at 1200 UTC, between two rainy events. It shows a progressive drying of the upper soil as it will be shown in the next section. The evolution of the different terms of the budget for the whole period is shown in Figure 2.

The turbulent fluxes are computed every 30 minutes using the eddy-correlation method with the standard corrections, the same used for all the equipments in BLLAST (Pietersen and De Coster, 2011), using the EC-pack (van Dijk et al., 2004) that
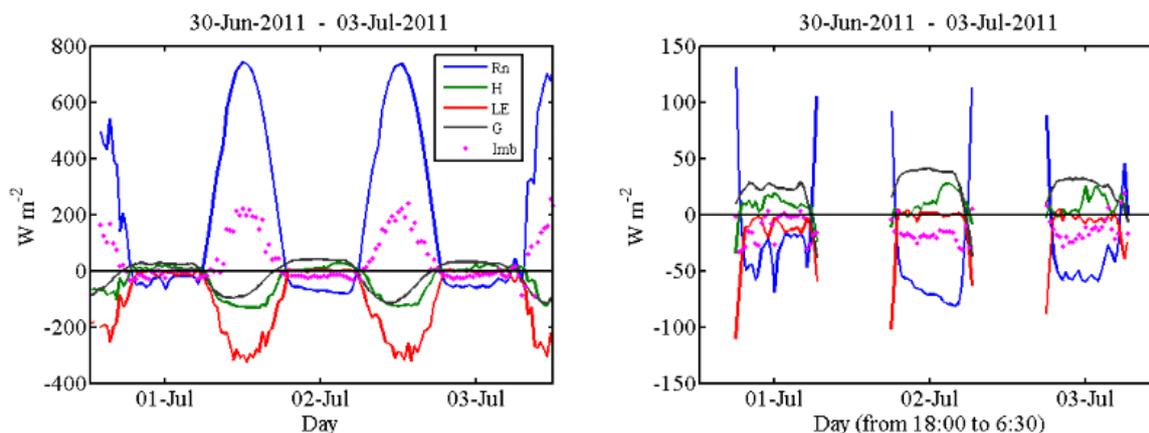
Figure 2. Surface energy budget in the small square for the period June 30 to July 3, between two rainy events (left), and zoom for the nighttime periods (right).

includes the computation of the planar fit angles to virtually rotate the sonic into the mean flow (Wilczak et al., 2001) and the Webb correction for the fluctuations of density (Webb et al, 1980).

The radiation term is the result of the budget of the four terms measured by the CNR1 (longwave and shortwave upward and downward fluxes). The ground flux is measured at 5 cm below the surface and corrected to the values at surface using the harmonic analysis (Heusinkveld et al., 2004) and simplifying the heat flux to a single sinusoidal function (Hillel, 1998), here resulting in an average increase of 40% of the value and a delay of 90 minutes.

Similarly to what is done in Cuxart et al. (2015), we consider positive terms those giving energy to the volume and negative those extracting energy from it. In this 72-hour series, shown in Figure 2, we see that in the daytime, Rn is the only input of energy and this energy is sent upward by turbulent latent and sensible fluxes and downward through the ground flux. However there is an excess of incoming energy that is not taken care of by these processes. This daytime imbalance is similar in magnitude to the latent heat flux, and larger than the sensible heat flux and the ground heat flux. In the small scale square, the amount of vegetation is small, so the B term is not important, neither are present any clear sources or sinks, or objects with storing capacity, meaning that S is also expected to be small. The tendency is found to be of the order of a few W m^{-2}. Therefore this imbalance larger than 100 W m^{-2} at the central hours of the day must be attributed to the advection term A or to other not accounted processes or factors Ot.

Figure 2 also displays a zoom of the budget for the three nights. Taking the second night for discussion, which is the one showing the most smooth time evolution, Rn is the largest term, now a loss, and the compensating heat fluxes are G and the H, whereas LE is very small. The imbalance is approximately one-fourth of Rn, around 20 W m^{-2}. In general terms, depending on the wind intensity, latent heat can release heat through condensation or capture it through evaporation. Again, since TT, B and S seem to be not relevant, the Imbalance should be explained either by A or Ot.

In the following sections we will explore, using the available modeling and observational information, what could be the order of magnitude of the values of the advection term in the SEB, making use of the observed horizontal temperature gradients in equation 4.

4 Estimation of the advection term at scales between 10 kilometers and the meter

4.1 Scales between 1 and 10 kilometers

The order of magnitude of the advection term at scales close to 1 kilometer or larger can be estimated using model outputs and satellite data. Green color in Figure 1 show the areas in domains D1 and D2 where the terrain has a height above sea level between 50 and 700 m. This allows avoiding coastal areas and mountainous terrain, so that the terrain complexity is comparable to the one around Lannemezan. The average values of LST and air temperature at some levels and the standard deviations are computed for these areas in green. The same statistics are computed from the available LST provided by MODIS (about 4 per day) and MSG (every 15min).
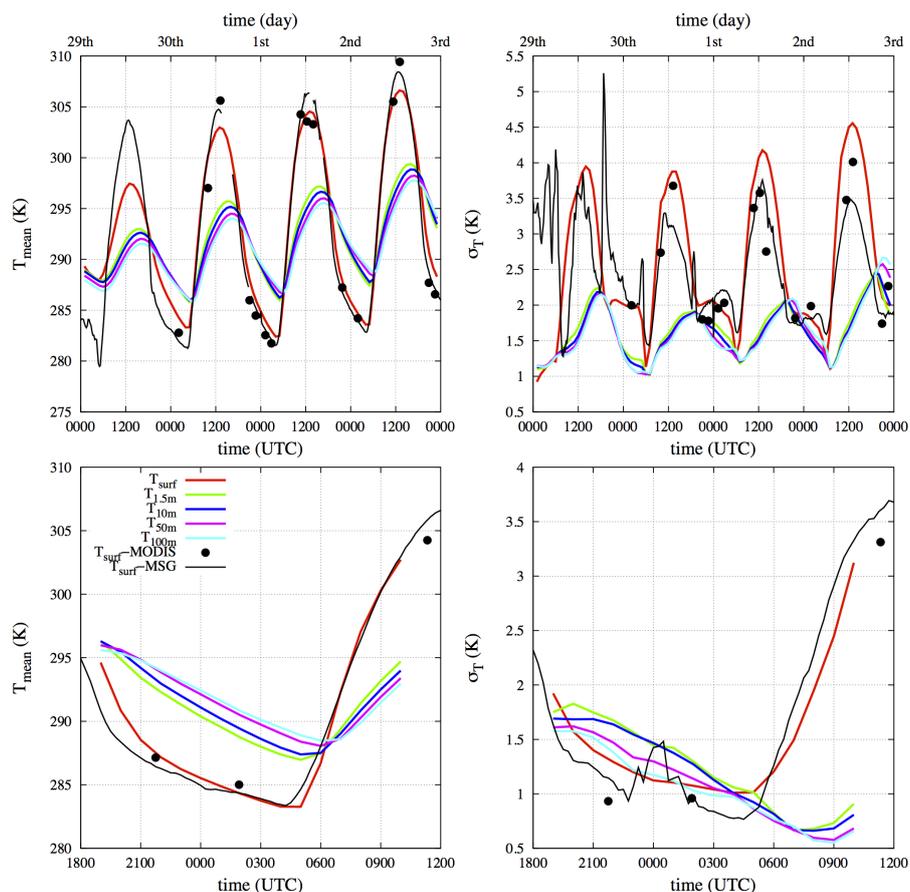
Figure 3. Top left: evolution of the average air temperature for some levels of the model and for the LST of the temperature, the available MODIS images and Meteosat Second Generation for D1 for a period of 5 days, Top right: standard deviation of the same variables of the large domain D1. Bottom left and right: as above for domain D2, which was run only for the night 2nd to 3rd July.

Figure 3 shows the evolution of the temperatures of the surface as seen by the model, MODIS on Aqua and Terra satellites, and SEVIRI on MSG for domains D1 and D2. Also the average values of the air temperature at 1.5, 10, 50 and 100 m above the surface are shown. It is noteworthy to point out that the close values of the model LST to the satellite values allow to use the model statistics with some confidence.

Focusing on the values of the standard deviation in Figure 3, we see that at a resolution at 2 km (D1) its value for the air temperature does not change with height, varying between 1 K and 2 K with maximal values in the afternoon and minimal at the end of the night. The LST variance is higher, with standard deviations around 3 K in the day and 2 K in the night, these values being given by the three different available sources (D1, MODIS and MSG). Taking the 1.5 m values of the standard deviation as an approximation to the typical changes of temperature over 2 km, the advection term according to equation 4 has a rough order of magnitude of less than 5 W m^{-2} both for night and day, for scales of 2 km or larger.

At the higher resolution run D2, we see that the standard deviation decreases with height, indicating that at this resolution the model is able to react significantly to the prescribed surface variability. The model has the largest values of the standard deviation for 1.5 m, varying between 0.7 and 1.8 K for the series shown. The corresponding rough order of magnitude according to equation 4 is of less than 10 W m^{-2}.

Therefore, for scales larger than 1 km the expected contribution of the advection term to the SEB would be of the order of 10 W m^{-2} in the daytime and of 5 W m^{-2} at night, but its relative contribution is much smaller for the daytime that for the night.
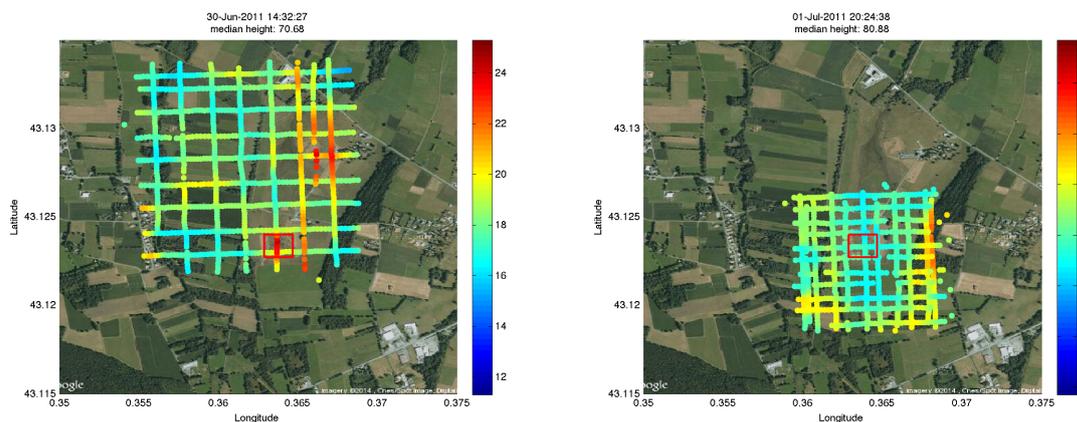
Figure 4. Surface temperature on June 30th, 2011 at 1432 UTC (left) and on July 1st at 2024 UTC (right) as measured by SUMO from an approximate height of 65 m AGL. The red rectangle indicates the position of the small square.

4.2 Scales under 1 kilometer

Small scale thermal heterogeneities may generate corresponding small scale circulations. If these patterns are shortly lived (few minutes) the corresponding circulations can be considered as turbulence, but if they are relatively persistent (longer than the averaging time for the computation of the turbulent fluxes) then these circulations can be considered as contributing to the advective term in the equation of T or, equivalently, in the SEB equation. Here we will analyze the variability of the temperature fields from the different available sources, and see how the advection term would behave at these fine scales.

4.2.1 The hectometer scale as seen by SUMO

As mentioned previously, SUMO flew at circa 65 m AGL, over a square of 1.6 km of side (the "SUMO square"), from sunrise to shortly after sunset. It provided, among other data, values of air temperature at that height and of LST, respectively at resolutions of 10 and 100 m, the latter with overlapping areas, always including the small scale square, with a flight duration typically of 10 minutes. Figure 4 shows two typical examples of the LST, one in the afternoon when the small square is warmer than its surroundings and one for the evening, when the small square is not showing a significant departure from the average value of the area. With the horizontal resolution of the IR-sensor being close to the size of the small scale heterogeneities site, the related thermal contrasts are probably underestimated.

If we split the measured LST in two categories, one from inside the small square and one from outside, we can compute thermal differences, as shown in Figure 5 left, the site becoming increasingly warmer during the first 5 hours of the day (up to 5 K), and the difference slowly decreasing afterwards during 10 hours until sunset, when it becomes negative and has values of about -1 K for the next hour. On the other hand, at a height near 65 m, the contrast is very weak or non-existing (Figure 5 right), showing that the effect of the thermal differences at the surface almost vanishes somewhere under this level.

If we estimate the order of magnitude of the advective term in the SEB (equation 4 using LST differences), the advection term takes values below $10\ Wm^{-2}$ just after sunrise and increases to about 60 W m^{-2} at the instant of maximum temperature difference between the square and the surroundings, slowly decreasing to about 10 W m^{-2} near sunset. These values may be overestimations since they have been computed using LST instead of the temperature of air at 2m.

It is also interesting to see if the standard deviation of LST ($\sigma(LST)$, Figure 6 left) for the complete SUMO square can be considered as an estimation of ΔT between the small square and its surroundings. Figures 5 left and 6 left show a similar behavior for both quantities, $\sigma(LST)$ being positive by definition, with comparable values. leading to similar estimations of A as just given. We will then, from now on, make the strong hypothesis that we may use $\sigma(LST)$ as a surrogate of ΔT, which may be acceptable since we are only estimating the order of magnitude of A, not intending to provide any precise values.
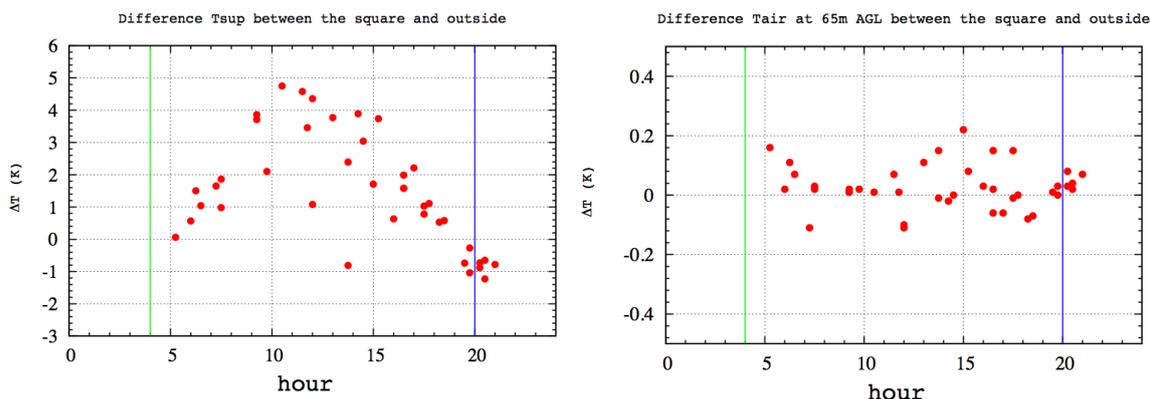
Figure 5. Difference for the SUMO square between the temperature inside and outside the small square for all flights during the whole BLLAST campaign, displayed by hour of the day for the LST (left) and the air temperature at circa 65 m AGL (right). Vertical lines indicate approximate sunrise (0420 UTC) and sunset (1940 UTC).
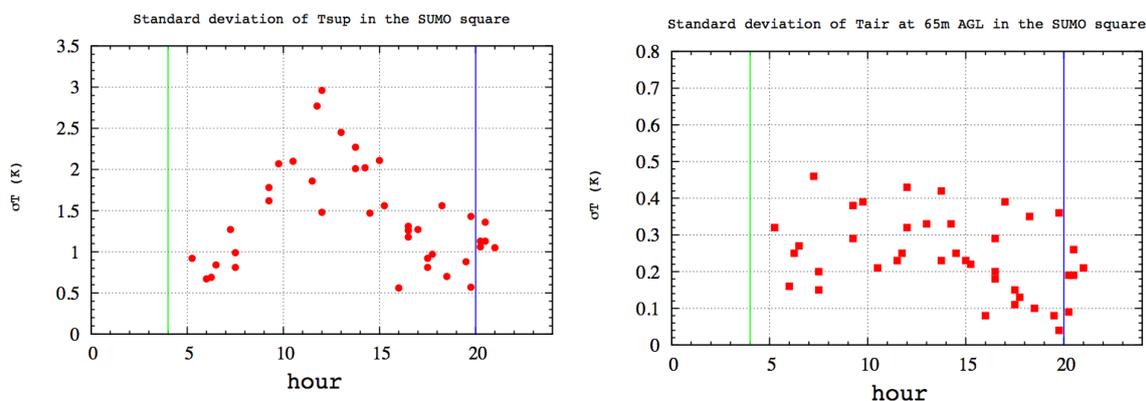
Figure 6. Standard deviation for the SUMO square for all flights during the whole BLLAST campaign, displayed by hour of the day for the LST (left) and the air temperature circa 65 m AGL (right). Vertical lines indicate sunrise (0420 UTC) and sunset (1940 UTC).

4.2.2 The hectometer scale as seen by the Meso-NH model

The Meso-NH model with domain D1, covering the Garonne basin and surroundings, has been run during four days of the
280 BLLAST campaign, whereas D2 and D3, covering respectively the Lannemezan plateau and surroundings and the SUMO square and surroundings have only been run for the night 1st to 2nd July due to the limitations of computational resources (D2 from 1800 UTC to 1000 UTC and D3 from 0000 UTC to 1000 UTC). Using a model at high-resolution has the advantage of having all the model information on the relevant variables, whereas the main disadvantage is the unavoidable departure from observations; in our case the variability of prescribed surface characteristics may be distant from reality.

285 The SUMO square is described by 25 model columns in D2 and by 441 model columns in D3 (D1 has not enough resolution to provide variability for the area). During the available hours for D2, $\sigma(LST)$ is close to 0.6K from sunset to late night and then falling to 0.3 K to shortly after sunrise. Then, in the morning hours it increases linearly to values close to 1.3 K at 10 UTC (Figure7 left). The behavior of D3 is similar at night, but after sunrise it allows for higher values (0.7 K) and the increase is slower having only 1 K at 10 UTC (Figure 7 right).

290 The variability for air temperature is explored taking four levels (1.5, 10, 50 and 100 m AGL) for every column of the SUMO square in both domains (FIgure 7). The standard deviation diminishes with height to values around 0.2 K at 50 m independently
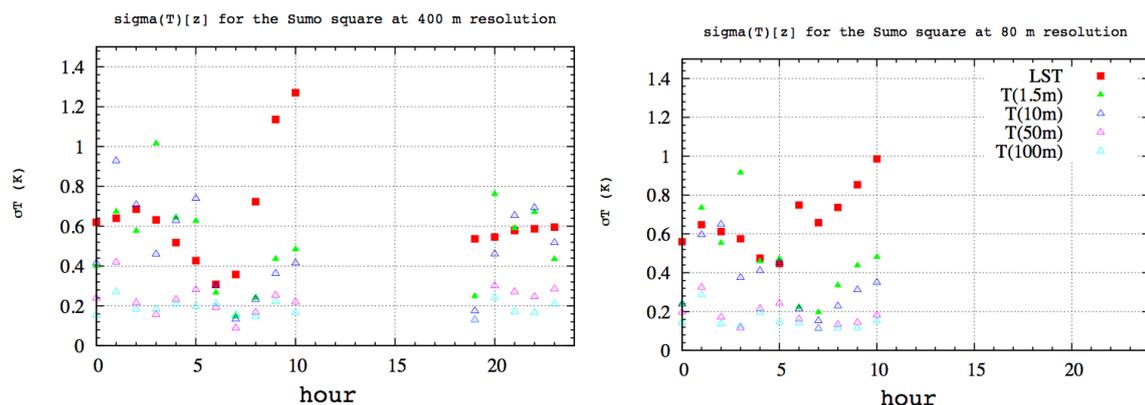
Figure 7. Evolution of the standard deviation of temperature for D2 (left, run only between July 1st at 1800 UTC and July 2nd at 1000 UTC) and for D3 (right, run only between 0000 and 1000 UTC of July 2nd)

of the hour, allowing to consider that the effect of the surface heterogeneities is mixed by convection in the daytime or does not reach these heights in the nighttime.

In the surface layer, represented here by the 1.5 and 10 m model levels, we see that the standard deviations are similar to the ones for the surface temperature in the nighttime (about 0.6 K) but significantly smaller in the daytime (0.4 K compared to about 1 K for the LST), when turbulence manages to reduce the differences effectively. This indicates that it is a fair approximation to take $\sigma(LST)$ as $\sigma(T)$ in the nighttime and in the morning and evening transitions, but that only half of its value should be taken in the daytime. From now on, based in these results we make the strong assumption that we can approximate the surface layer temperature variability to the one of the LST, which is possible in the frame of this study due to our aim to simply provide estimates of the order of magnitude of A.

Therefore, estimating the advection terms with these standard deviations (taking 0.5 K for the whole day in both domains) we get values of the order of 2 Wm^{-2} for the larger domain and of order of 15 Wm^{-2} for the smaller domain, due to the decreasing value of Δx. D3 provides values comparable to the ones computed from the SUMO at night and smaller during the day. Probably these values are also underestimated due to lesser variability in the model surface than in reality.

4.2.3   The decameter resolution estimated using soil moisture measurements

In several days during BLLAST, instantaneous point measurements of superficial soil moisture (SM) were made inside the small square using manual Delta-T devices, that provided an integrated value for the layer between the surface and -5 cm. For each measuring spot, several measurements were taken in an area of about 2 meters of radius, and the average value was saved. Variability at this fine scale was high (Evett et al, 2006). The square had a very gentle slope (less than 1%) towards the SW corner, where rain water tended to accumulate superficially. Some areas of the square had bare soil, but most of the area was covered by grass (alive and dead) with small bare spots in between.

Figure 8 shows the progressive and inhomogeneous drying over the square for three days after the rainy event of June 29. The day after the rain (30th) most of the square has values of SM above 30% increasing westwards to more than 40% and with water over the ground in the SW corner, with SM close to 60%. The second day (July 1st) there is a progressive drying and the bare soil areas at the E decrease their SM to values below 20%, whereas the W part has values between 25 and 60%. These heterogeneities imply very different values locally of the Bowen ratio and of the surface temperature. In the third day (July 2nd) drying continues, but the surface variability is similar along the square.

This information is not transported into any quantitative estimation - this will be done in the next subsections using IR sensors. However it may be induced from it that heterogeneities at the decameter scale are large and of longer timescale that the turbulent motions. They may force a relatively steady distribution of eddies inside the square, diminishing the representativity of any point measurement within it.
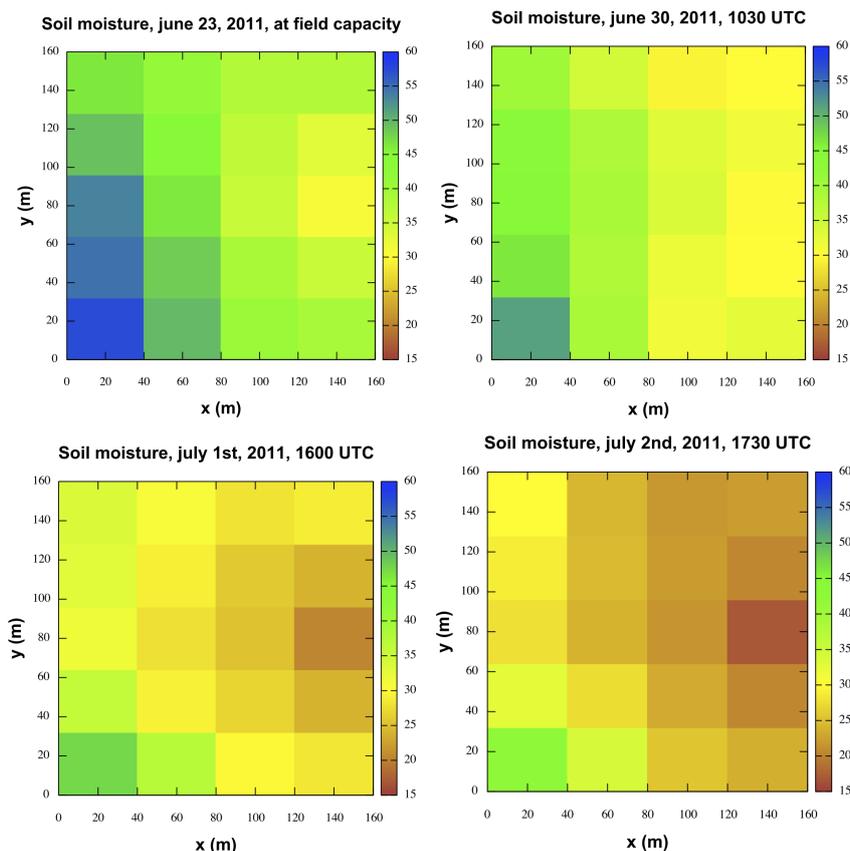
Figure 8. Maps of the soil moisture (first 5 cm) in the small square derived from point measurements from June 30 to July 2nd. Measurement at June 23rd is included for reference, since that day the terrain was at field capacity.

4.2.4 The decameter resolution as sampled with the multicopter

The OWL multicopter flew over the small square in the period 1 to 5 July at different times of the day. Flights were of short duration (several minutes) and consisted in horizontal transects at an approximate height of 5 m. In addition, some vertical profiles were made, up to about 30 meters a.g.l. over some selected points. The spatial resolution of the LST measurements from this height, with a cone of view of the IR sensor of 40° is around 5 m, and the fact that the flights have some inclination in respect to the horizontal make 10 m as a safer estimation. The air temperature is sampled at 1 Hz, equivalent to a spatial resolution of a few meters.

Figure 9 displays the standard deviations of the air and the surface temperature as a function of the hour of the day, for all flights of all five days. The values for LST are between 0.5 and 1 K at late night and the morning transition, they increase to 3.5 K during the morning decreasing afterwards to values essentially between 1 and 2 K in the evening transition. The pattern is very similar to what has been found from the model and the SUMO data, but the values are larger except for the late night and morning transition. Some large values of $\sigma(LST)$ just before the sunset are noteworthy.

Here $\sigma(T(5m))$ has the particularity that it is obtained at levels that can be readily compared to model data at 10 m. The model was providing values of $\sigma(T)$ of the order of 0.5 K for D3, and the multicopter is providing values of the same order in the daytime and close to 0.3 K in the nighttime and the transitions. The profiles shown in Figure 9 show that the variability in this afternoon case are of the order of 1-2 K, whereas the few available night profiles (not shown) present differences of some tenths of K, comparable to the respective $\sigma(LST)$. As an example of the method, LST and T(5m) transsects are also displayed
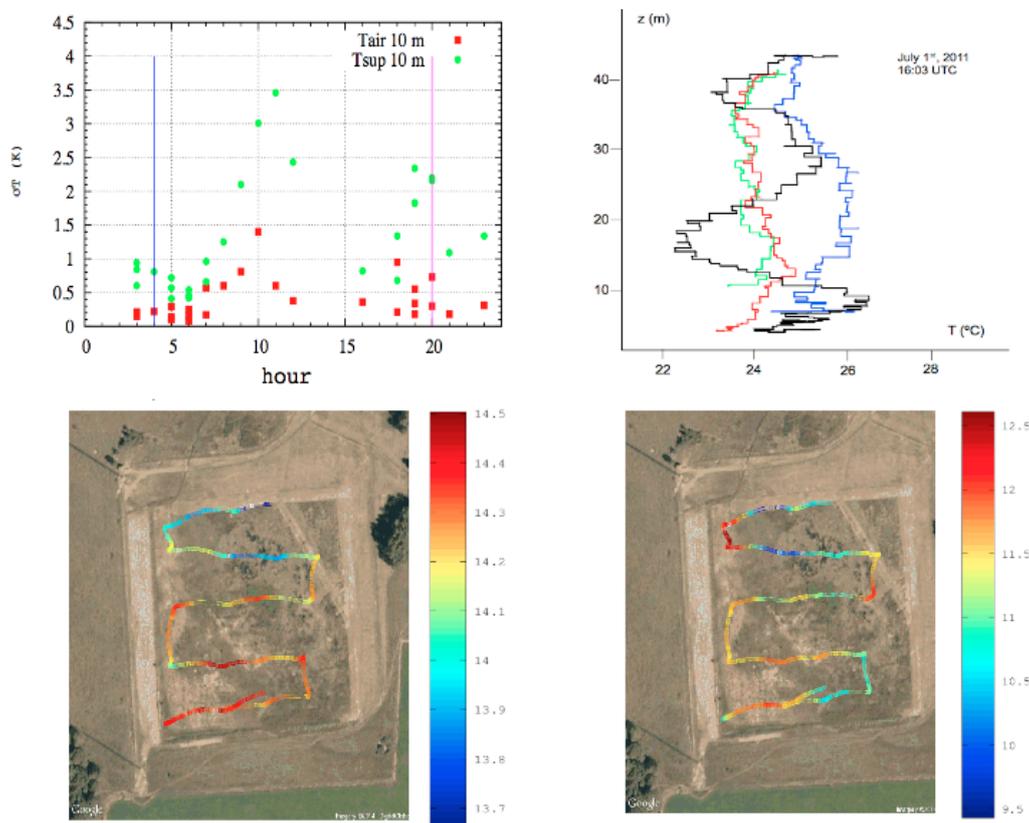
Figure 9. Multicopter: LST and air temperature standard deviation for the small square for the ensemble of flights during 5 days, blue and purple lines indicating respectively sunrise and sunset times (top left); vertical profiles inside the small square in the afternoon, made within 5 minutes (top right). Nocturnal flight pattern and LST values (bottom left) and air temperature at 5 m a.g.l. (bottom right).

in Figure 9 for a late night flight, and we can see that surface and 5 m temperatures show similar patterns of variability, the latter having a smaller amplitude.

If we translate these estimations of $\sigma(T)$ into the advection term, they provide values larger than for the hectometer scales, because they take place on smaller scales Δx. If we just take 0.5 K for the day and 0.2 K for the night, the corresponding advection values would be 100 and 40 Wm^{-2}. It is not possible to know at this stage if these thermal differences are transient, and therefore their effects taken into account in the turbulence fluxes, or more sustained in time, although the latter case seems not likely.

4.2.5 The meter resolution as seen by thermal imagery

IR sensor at 1.5 m AGL: Figure 10 left displays an image taken with the WUR IR Snapshot camera over a grass area in the small square. This surface typically contains green grass, dead grass and some small spots of bare soil, a typical example of the surface of the area. LST is patchy with up to 2K variations in less than 1 m of distance. In Figure 10 right, it can be seen that the standard deviation of LST is of the order of 0.5 K regardless of the type of surface inspected and if there is daytime and with clear skies (measurements between minutes 00 and 33) or cloudy at nighttime (from minute 64). Probably no organization of the flow can exist at such small scales, but associated microcirculations could exist that would break homogeneity, which may be a key factor in the night, being a factor that may oppose to runaway cooling as it is experienced in some numerical models.

IR sensor at 50 m AGL: The USDC IR sensor pointing at the NW corner of the small square is providing LST fields at a spatial resolution of 0.4 m x 0.2 m approximately. As indicated in the analysis of the overall results in Garai and Kleissi (2013), the average value of the standard deviation for this area is around 0.3 K for 30-min averaging period. They report that,
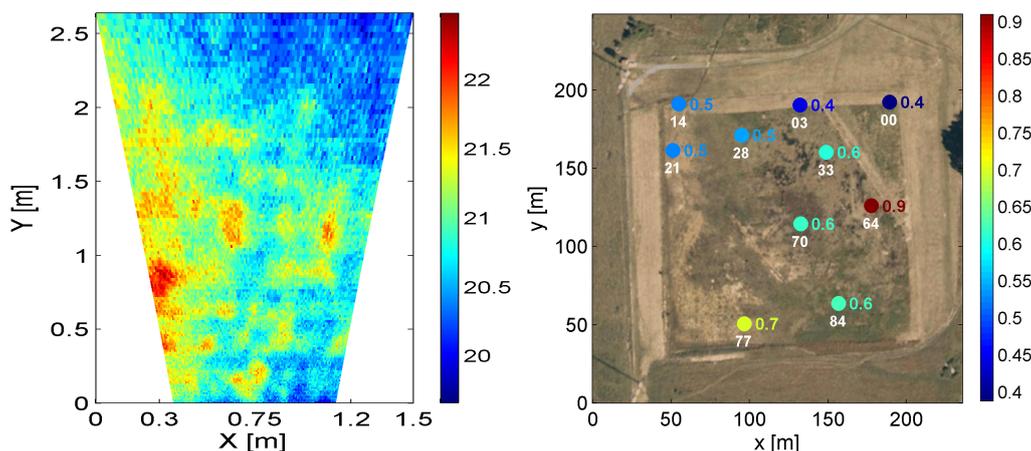
Figure 10. Variability inside a WUR IR image for a grass area at 1820 UTC of June 21st (left); standard deviation of LST for 10 similar measurements in the small square from a height of 1.5 m AGL during the evening of the same day, the numbers in white are minutes from the start of measurements, those made after minute 33 were after sunset (right).
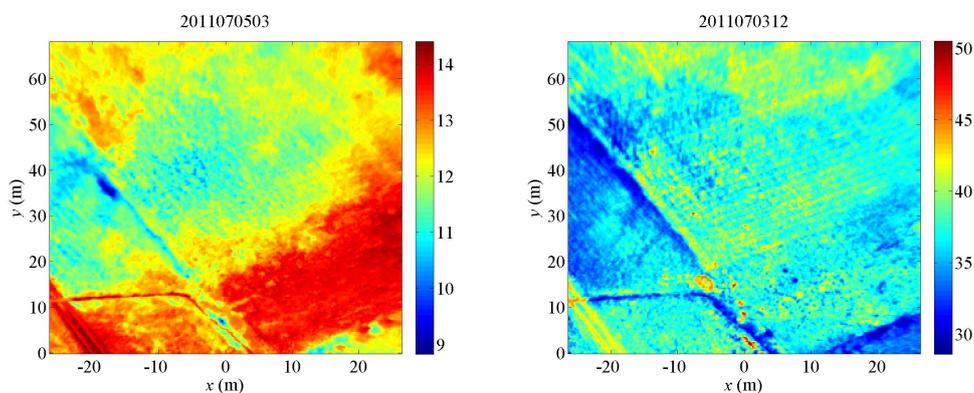
Figure 11. NW corner of the small square as seen from a IR camera of the UCSD at 50 m at 03 UTC of July 5th (left) and 12 UTC (right) of July 3rd, 2011. The picture is oriented in a way that the top part looks to SE.

in the daytime, the high and low temperature structures seem to be highly correlated with ejection and sweep events. Figure 11 displays one image at night of July 5th and one at noon of July 3rd. The night image shows that in the small square (tones yellow to blue) there are variations of 1-2 K at several scales, whereas the warm area in red outside the square may induce for this night a larger circulation. During the day, the amplitude of the differences is larger (of the order of 5 K) and the patches seem to be of smaller scale.

5   Discussion

To help making a compact discussion, a summary of the previous results is given in Table I. We estimate the gradient of temperature $\Delta T/\Delta x$ as $\sigma(T)/r$, where r stands for the resolution. As described, two strong hypotheses are behind this approximation. Firstly, we can use $\sigma(T)$ as a surrogate for ΔT which is based on the comparison of Figures 5 left and 6 left, which show that the time evolution and amplitude of $\sigma(T)$ for the SUMO square compare well with ΔT between the small square and the rest of the SUMO square.

Secondly, as seen in Fig 3 bottom right for the 400 m resolution run of Meso-NH and, more clearly, in Figure 9 top-left, when comparing the standard deviations of the air temperature at the surface layer and of LST obtained by the multicopter on the small square, it is legitimate to assume that the standard deviation of these quantities (temperature of air in the surface layer and LST) have values of the same order of magnitude. These approximations exclude that we can provide meaningful values for the advection term A of the SEB, but it allows to estimate generic orders of magnitude, which is a first step towards the increase of understanding. A final reminder is that the mean vertical velocity at the temporal scale of our SEB (30-minute averages) is taken as zero, therefore any vertical advection is neglected and will be accounted implicitly in the term Ot of equation (2).

Table 1. Estimation of the order of magnitude of the advection term A in the Surface Energy Budget equation, for different sources and scales, taking 200 W m^{-2} as imbalance at the center of the day (D) and 30 W m^{-2} at night (N). The orders of magnitude are rounded, as are the percents of the imbalance.

Source	Scale r (m)	D/N	$\sigma(T)(K)$	$O(\sigma(T)/r)(K/m)$	$O(Adv(T))(W\,m^{-2})$	% Imb
Model D1 and MSG	4000	D	2	0.0005	1	0.5
		N	1	0.0002	0.5	2
Model D2 and MODIS	1000	D	1.5	0.0015	5	3
		N	1	0.0010	5	10
Model D3	200	D	0.5	0.0025	5	5
		N	0.5	0.0025	5	20
SUMO	100	D	1.5	0.0150	40	20
		N	0.5	0.0050	10	30
Multicopter	10	D	0.5	0.0500	125	60
		N	0.1	0.0100	25	80
Thermal cameras	1	D	0.5	0.5000	1250	600
		N	0.1	0.1000	250	800

One obvious result is that the order of magnitude of the advection term increases as the scale becomes finer. Therefore the usual assumption that this term is very small compared to the main ones of the SEB equation stands for scales as fine as one kilometer or broader. This is in agreement with the previous argumentations of Foken (2008) and Leuning et al (2012), that indicated that the advection term was not large enough to explain a substantial part of the imbalance in the measured SEB using only the 4 main terms (equation 1).

When the attention is turned to the smallest scales as the ones provided by the thermal cameras, of the order of 1 m, we see that the standard deviation of the surface temperature is of the same order as at larger scales, providing very high estimations of the advection term. In fact, Mahrt (2000) indicates that these heterogeneities may be restricted to the roughness sublayer ("the layer below the surface layer") that extends to the blending height, above which the effect of this small-scale heterogeneities is perceived as integrated by the surface layer. In the roughness layer, typically of the order of magnitude of the roughness elements of the surface, Monin-Obukhov similarity is not applicable because the turbulence is not in equilibrium with the local gradient. These roughness elements are of the order of few centimeters in most of the small scale.

This allows to exclude from our analysis the heterogeneity of very small scale as detected by the thermal cameras that, in fact, overpass by far the values of the imbalances at day and at night. In practical terms, it also means that these thermal differences in the roughness layer do not manage to organize persistent circulations at the level of the measuring screen. Instead, the persistence of such heterogeneities may indicate that circulations at the centimeter or decimeter scales very close to the ground may establish, which could contribute to the fact that the surface does not experience nocturnal runaway cooling, contrarily to what models generate in flat areas that they treat as homogeneous. This subject should be explored further in an independent research action.

Therefore the most relevant range of scales is the one comprising the hectometer and the decameter scales. The former ones correspond to the actual scales of landscape heterogeneities in the area, such as crop fields and wooden areas in between, or farms and small villages. Even the town of Lannemezan has a characteristic size smaller than one kilometer. These patterns are either permanent (wooden areas, farms and villages) or slowly varying with the seasons (crops and grass lands). That is, these heterogeneities are fixed at the daily scale, and generate circulations that may persist for several hours and cannot be treated as turbulence. The estimations provided by the model and the SUMO indicate that these circulations may easily account for advections of the order of 10 W m^{-2} that explain less than 10 % of the imbalance in the daytime, but may be or the order of 30% in the nighttime, and as large as the other main terms in equations (1) and (2).

The scales of the order of the decameter, illustrated here with the multicopter data, indicate that the heterogeneities are large in the daytime, very much in accordance with the picture provided by LES and DNS of the Convective Boundary Layer, where

405   small plumes exist everywhere in the first 10 m above the ground and only a few plumes (at a scale close to 100 m) manage to grow and make part of the Mixed Layer. It is difficult then to consider conceptually this variability as a contribution to the advection term, although there is no reason not to be able to compute the advection term, and in fact it may be behind some of the imbalance, explaining some tens of W m^{-2} in the daytime.

    The heterogeneities in the surface temperature at the decameter scale in the nighttime as seen by the multicopter are weak,
410   of the order of 0.2 K, a value that we considered not relevant when found for the air temperature at 65 m as sampled by the SUMO. Therefore, even if the estimated advection term is of the order of 50 W m^{-2}, and could explain a largely the imbalance, we prefer to refrain to make any strong statement about this issue due to the few data available at night and conclude that more measurements are needed, perhaps pointing to the fact that these scales may generate motions that could be included in the turbulence fluxes.

415   As the main point, it seems relevant to state that for scales of the order of hectometers, the circulations generated by the surface heterogeneities may be relatively persistent and explain a substantial part of the imbalance in the SEB, especially at night. For larger scales the contributions are small and for finer scales the subject is still open to discussion, but probably these motions are small and restricted to very close to the surface. Since the surface temperature field seems to have a variability close to the one of air temperature at the screen level, a possible estimation of the contribution of the subgrid or subpixel
420   variability to the SEB might be provided using $\sigma(LST)$ from satellite images in the approximate equation (4).

6   Conclusions

This work has explored the order of magnitude of the advection term in the SEB using a number of sources, including model outputs at different resolutions, satellite images, remotely-controlled measuring devices (SUMO and multicopter) and thermal cameras. The SEB is computed using the measurements on a small squared area in BLLAST, which provides an estimation
425   of the imbalances, which is of the order of 200 W m^{-2} in the central part of the day, and close to 30 W m^{-2} at night, both values being very similar to the ones of the turbulent sensible and latent heat fluxes and of the ground flux, at day and night respectively.

    The variability of the surface temperature fields as provided by the different sources has been explored and it has been compared with the variability of the air temperatures in the surface when possible. It is seen that this variability has similar
430   values for all the scales inspected, implying that the advection term is increasingly larger as the scale becomes finer. The variability of the air temperature close to the surface is similar to the one of the surface, using the information that we have, essentially from the model outputs and the multicopter transects.

    The advection term corresponding to scales above the kilometer are much smaller than the other terms and cannot explain any significant part of the imbalance, either because there are no real circulations performing the transport or because the steady
435   state regime makes the net advection very small. On the other extreme of the spectrum of scales, those of the order of the meter still show very significant temperature variability, but the associated values of advection are too high to be meaningful, and probably are related to redistribution of heat in the first centimeters above the surface within the conceptual box of computation of the SEB and therefore not relevant for the SEB.

    The hectometer scale generating motions that last longer than the averaging time of the turbulent fluxes, linked to terrain
440   heterogeneities may explain significant parts of the imbalance. To this we may add the contribution of smaller scales, but it is a matter of discussion if these decameter scales are to be considered in the advection term or in the turbulence term. A first estimation of the value of the advection term in the SEB may be given by equation (4), using as a surrogate of the temperature increments of the surface layer the standard deviation of the land surface temperature as provided by satellites or even the outputs of a numerical model, but this should be the subject of further experimentation.

445   *Acknowledgements.* BLLAST field experiment was made possible thanks to the contribution of several institutions and supports: INSU-CNRS (Institut National des Sciences de l'Univers, Centre National de la Recherche Scientifique, LEFE-IDAO program), Météo-France, Observatoire Midi-Pyrénées (University de Toulouse), EUFAR (EUropean Facility for Airborne Research) and COST ES0802 (European Cooperation in the field of Scientific and Technical). The field experiment would not have occurred without the contribution of all participating European and American research groups, which have all contributed in a significant amount (see supports). BLLAST field experiment
450   was hosted by the instrumented site of Centre de Recherches Atmosphériques, Lannemezan, France (Observatoire Midi-Pyrénées, Laboratoire d'Aérologie). BLLAST data are managed by SEDOO, from Observatoire Midi-Pyrénées. We wish to particularly acknowledge Felipe Molinos, who assisted the University of the Balearic Islands team in the field, and the students of the Wageningen University that took the pictures with the thermal camera, specially Linda Kooijmans and Daniel Kunne. ECMWF and AEMET have provided computing time through the research project "Effect of the surface heterogeneities in the atmospheric boundary layer". The Spanish Ministry of Research
455   has partially funded this action through grants CGL2009-12797-C03-01, CGL2012-37416-C04-01, supplemented with FEDER funds, and PCIN-2014-016-C07-01, part of a ERA-Net + of the European Union.

References

Cuxart, J., Bougeault, P., Redelsperger, J. L. (2000). A turbulence scheme allowing for mesoscale and large?eddy simulations. Quarterly Journal of the Royal Meteorological Society, 126(562), 1-30.

Cuxart, J., Conangla, L., Jiménez, M. A. (2015). Evaluation of the surface energy budget equation with experimental data and the ECMWF model in the Ebro Valley. Journal of Geophysical Research: Atmospheres, 120(3), 1008-1022.

De Coster, O. , Pietersen, H.P., 2011: BLLAST-uniform processing of Eddy-Covariance data, Master Thesis report, Université de Toulouse (France).

Evett, S. R., Tolk, J. A., Howell, T. A. (2006). Soil profile water content determination. Vadose Zone Journal, 5(3), 894-907.

Foken, T, (2008a): Micrometeorology, Springer Science and Business Media.

Foken, T. (2008b). The energy balance closure problem: an overview. Ecological Applications, 18(6), 1351-1367.

Foken, T., Leclerc, M. Y. (2004). Methods and limitations in validation of footprint models. Agricultural and Forest Meteorology, 127(3), 223-234.

Garai, A., Kleissl, J. (2013). Interaction between coherent structures and surface temperature and its effect on ground heat flux in an unstably stratified boundary layer. Journal of Turbulence, 14(8), 1-23.

Hartogensis, O (2015): BLLAST Flux Maps. 6th BLLAST workshop, Barcelona, 2-3 February 2015.

Heusinkveld, B. G., Jacobs, A. F. G., Holtslag, A. A. M., Berkowicz, S. M. (2004). Surface energy balance closure in an arid region: role of soil heat flux. Agricultural and Forest Meteorology, 122(1), 21-37.

Hillel, D., 1998: Environmental soil physics: Fundamentals, applications, and environmental considerations. 771 pp.

Jiménez, M. A., Cuxart, J. (2014). A study of the nocturnal flows generated in the north side of the Pyrénées. Atmospheric Research, 145, 244-254.

Lafore, J. P., Stein, J., Asencio, N., Bougeault, P., Ducrocq, V., Duron, J., ... Pinty, J. P. (1997). The Meso-NH atmospheric simulation system. Part I: adiabatic formulation and control simulations. In Annales Geophysicae (Vol. 16, No. 1, pp. 90-109). Springer-Verlag.

Leuning, R., Van Gorsel, E., Massman, W. J., Isaac, P. R. (2012). Reflections on the surface energy imbalance problem. Agricultural and Forest Meteorology, 156, 65-74.

Lothon, M., Lohou, F., Pino, D., Couvreux, F., Pardyjak, E. R., Reuder, J., ... Augustin, P. (2014). The BLLAST field experiment: Boundary-layer late afternoon and sunset turbulence. Atmospheric chemistry and physics, 14(20), 10931-10960.

Mahrt, L. (2000). Surface heterogeneity and vertical structure of the boundary layer. Boundary-Layer Meteorology, 96(1-2), 33-62.

Martínez, D., Jiménez, M. A., Cuxart, J., Mahrt, L. (2010). Heterogeneous nocturnal cooling in a large basin under very stable conditions. Boundary-Layer meteorology, 137(1), 97-113.

Morcrette, J. J. (1990). Impact of changes to the radiation transfer parameterizations plus cloud optical. Properties in the ECMWF model. Monthly Weather Review, 118(4), 847-873.

Noilhan, J., Planton, S. (1989). A simple parameterization of land surface processes for meteorological models. Monthly Weather Review, 117(3), 536-549.

Oke, T. R. (1987). Boundary layer climates. Routledge.

Oncley, S. P., Foken, T., Vogt, R., Kohsiek, W., DeBruin, H. A. R., Bernhofer, C., ... Lehner, I. (2007). The energy balance experiment EBEX-2000. Part I: overview and energy balance. Boundary-Layer Meteorology, 123(1), 1-28.

Reuder, J., Brisset, P., Jonassen, M., Muller, M., Mayer, S. (2009). The Small Unmanned Meteorological Observer SUMO: A new tool for atmospheric boundary layer research. Meteorologische Zeitschrift, 18(2), 141-147.

Reuder and Jonassen (2012) : "First Results of Turbulence Measurements in a Wind Park with the Small Unmanned Meteorological Observer SUMO"; Energy Procedia, Volume 24, Pages 176-185.

Salomonson, V.V., Bames, W.L., Maymon, W.P., Montgomery, H., 1989. MODIS: advanced facility instrument for studies of the Earth as a system. IEEE Trans. Geosci. Remote Sens. 27, 145-153.

Schmetz, J., Pili, P., Tjemkes, S., Just, D., Kerkmann, J., Rota, S., Ratier, A., 2002. An introduction to Meteosat Second Generation (MSG). Bull. Amer. Meteor. Soc. 83, 977-992.

Van de Boer, A., Moene, A. F., Graf, A., Schuttemeyer, D., Simmer, C. (2014). Detection of Entrainment Influences on Surface-Layer Measurements and Extension of Monin-Obukhov Similarity Theory. Boundary-Layer meteorology, 152(1), 19-44.

Van Dijk, A., Moene, A.F., and De Bruin, H.A.R., 2004: The principles of surface flux physics: theory, practice and description of the ECPACK library, Internal Report 2004/1, Meteorology and Air Quality Group, Wageningen University, Wageningen, the Netherlands, 99 pp.

Webb, E. K., Pearman, G. I. and Leuning, R. (1980), Correction of flux measurements for density effects due to heat and water vapour transfer. Q.J.R. Meteorol. Soc., 106: 85-100. doi: 10.1002/qj.49710644707

Wilczak, J. M., Oncley, S. P., Stage, S. A. (2001). Sonic anemometer tilt correction algorithms. Boundary-Layer Meteorology, 99(1), 127-150.

Wrenger, B., Dunnermann, J., Cuxart, J., Palau, J.L. (2013), Sampling the establishment of the nocturnal inversion with a multicopter, 1st ISARRA workshop, Palma de Mallorca (Spain), 18-20 February 2013.